In practice the molecules perform more or less finite librations about the main orientation. The structure factor may then be found by the method of symmetry-adapted functions [see, *e.g.*, Press (1973), Press & Hüller (1973), Dolling *et al.* (1979), Prandl (1981, and references therein)].

$$\langle F\rangle = \sum_k f_k 4\pi \sum_\nu \sum_{\mu=-\nu}^{+\nu} i^\nu j_\nu(\mathbf{H}\cdot\mathbf{r}_k) C_{\nu\mu}^{(k)} Y_{\nu\mu}(\theta,\varphi). \qquad (4.2.4.98)$$

$j_\nu(z)$ is the νth order of spherical Bessel functions, the coefficients $C_{\nu\mu}^{(k)}$ characterize the angular distribution of $\mathbf{r}_k$, $Y(\theta,\varphi)$ are the spherical harmonics where $|\mathbf{H}|,\theta,\varphi$ denote polar coordinates of $\mathbf{H}$.

The general case of an arbitrary crystal, site and molecular symmetry and the case of several symmetrically equivalent orientationally disordered molecules per unit cell are treated by Prandl (1981); an example is given by Hohlwein *et al.* (1986). As mentioned above, cubic plastic crystals are common and therefore mostly studied up to now. The expression for $\langle F\rangle$ may then be formulated as an expansion in cubic harmonics, $K_{\nu\mu}(\theta,\varphi)$:

$$\langle F\rangle = \sum_k f_k 4\pi \sum_\nu \sum_\mu i^\nu j_\nu(\mathbf{H}\cdot\mathbf{r}_k) C_{\nu\mu}^{\prime(k)} K_{\nu\mu}(\theta,\varphi). \qquad (4.2.4.99)$$

($C'_{\nu\mu}$ are modified expansion coefficients.)

Taking into account isotropic centre-of-mass translational displacements, which are not correlated with the librations, we obtain:

$$\langle F'\rangle = \langle F\rangle \exp\{-\tfrac{1}{6}H^2\langle U^2\rangle\}. \qquad (4.2.4.100)$$

U is the mean-square translational displacement of the molecule. Correlations between translational and vibrational displacements are treated by Press *et al.* (1979).

Equivalent expressions for crystals with symmetry other than cubic may be found from the same concept of symmetry-adapted functions [tables are given by Bradley & Cracknell (1972)].

4.2.4.5.3. *Short-range correlations*

The final terms in equations (4.2.4.90) and (4.2.4.93) concern correlations between the orientations of different molecules. Detailed evaluations need a knowledge of a particular model. Examples are compounds with nitrate groups (Wong *et al.*, 1984; Lefebvre *et al.*, 1984), CBr_4 (More *et al.*, 1980, 1984), and many others (see Sherwood, 1979). The situation is even more complicated when a modulation wave with respect to the occupation of different molecular orientations is superimposed. A limiting case would be a box-like function describing a pattern of domains. Within one domain all molecules have the same orientation. This situation is common in ferroelectrics where molecules exhibit a permanent dipole moment. The modulation may occur in one or more directions in space. The observed intensity in this type of orientationally disordered crystal is characterized by a system of more or less diffuse satellite reflections. The general scattering theory of a crystal with occupational modulation waves follows the same lines as outlined in Section 4.2.3.1.

4.2.5. Measurement of diffuse scattering

To conclude this chapter experimental aspects are summarized which are specifically important in diffuse-scattering work. The summary is restricted to film methods commonly used in laboratories and (X-ray or neutron) diffractometer measurements. Sophisticated special techniques and instruments at synchrotron facilities and reactors dedicated to diffuse-scattering work are not described here. The full merit of these machines may be assessed after inspection of corresponding user handbooks which are available upon request. Also excluded from this section are instruments and methods related to diffuse scattering at low angles, *i.e.* small-angle scattering techniques. Although no fundamental differences exist between an X-ray experiment in a laboratory and at a synchrotron facility, some specific points have to be considered in the latter case. These are discussed by Matsubara & Georgopoulos (1985), Oshima & Harada (1986), and Ohshima *et al.* (1986).

Generally, diffuse scattering is weak in comparison with Bragg scattering, anisotropically and inhomogeneously distributed in reciprocal space, elastic, inelastic, or quasi-elastic in origin. It is frequently related to more than one structural element, which means that different parts may show different behaviour in reciprocal space and/or on an energy scale. Therefore special care has to be taken concerning the following points: (1) type of experiment: X-rays or neutrons, film or diffractometer/spectrometer, single crystal or powder; (2) strong sources; (3) best choice of wavelength (or energy) of incident radiation if no 'white' technique is used; (4) monochromatic and focusing techniques; (5) sample environment and background reduction; (6) resolution and scanning procedure in diffractometer or densitometer recording.

On undertaking an investigation of a disorder problem by an analysis of the diffuse scattering an overall picture should first be recorded by X-ray diffraction experiments. Several sections through reciprocal space help to define the problem. For this purpose film methods are preferable. Cameras with relatively short crystal–film distances avoid long exposure times. Unfortunately, there are some disorder problems which cannot be tackled by X-ray methods. X-rays are rather insensitive for the elucidation of disorder problems where light atoms in the presence of heavy atoms play the dominant role, or when elements are involved which scarcely differ in X-ray scattering amplitudes (*e.g.* Al/Si/Mg). In these cases neutrons have to be used at an early stage. If a significant part of the diffuse scattering is suspected not to be of static origin concomitant purely elastic, quasi-elastic or inelastic neutron experiments have to be planned from the very beginning.

Because diffuse scattering is usually weak, intense radiation sources are needed, whereas the background level should be kept as low as possible. Coming to the background problem later, we should make some brief remarks concerning sources. Even a normal modern X-ray tube is a stronger source, defined by the flux density from an anode (number of photons $cm^{-2}\ s^{-1}$), than a reactor with the highest available flux. For this reason most experimental work which can be performed with X-rays should be. Generally the characteristic spectrum will be used, but special methods have been developed where the white X-ray spectrum is of interest (see below). A most powerful source in this respect is a modern synchrotron storage ring (see, *e.g.*, Kunz, 1979). With respect to rotating anodes one should bear in mind not only the power but also the flux density, because there is little merit for a broad focus in diffuse-scattering work (separation of sharp and diffuse scattering). One can suppose that synchrotron radiation in the X-ray range will also play an important role in the field of monochromatic diffraction methods, owing to the extremely high brilliance of these sources (number of quanta cm^{-2}, sr^{-1}, s^{-1} and wavelength interval). Diffuse neutron-diffraction work may only be performed on a high- or medium-flux reactor. Highly efficient monochromator systems are necessary. In combination with time-of-flight neutron methods pulsed sources are nowadays equivalent to reactors (Windsor, 1982).

If film and (X-ray) diffractometer methods are compared, film techniques are highly recommended at an early stage to give a general survey of the disorder problem. Routine X-ray techniques such as rotation photographs, Weissenberg or precession techniques may be used. The Weissenberg method is preferred to the

precession method in most cases because of the comparatively larger coverage of reciprocal space (with the same wavelength). The drawback of a distorted image of the reciprocal space may be compensated by digitizing the film blackening *via* a densitometer recording and subsequent plotting. With this procedure a distorted section through the reciprocal lattice may be transformed into a form suitable for easy interpretation (Welberry, 1983).

Frequently used are standing-crystal techniques in combination with monochromatic radiation, usually called monochromatic Laue techniques (see, *e.g.*, Flack, 1970). The Noromosic technique (Jagodzinski & Korekawa, 1973) is characterized by a convergent monochromatic beam which simulates an oscillation photograph over a small angular range. Heavily overexposed photographs, with respect to Bragg scattering, allow for sampling of diffuse intensity if a crystal is oriented in such a way that there is a well defined section between the Ewald sphere and the diffuse phenomenon under consideration. By combining single Noromosic photographs, Weissenberg patterns can be simulated. This relatively tedious way of comparison with a true Weissenberg photograph is often unavoidable because the heavily overexposed Bragg peaks obscure weak diffuse phenomena over a considerable area of a photograph. Furthermore, standing pictures are pointwise measurements in comparison with the normal continuous pattern with respect to the crystal setting. Long-exposure Weissenberg photographs are therefore not equivalent to a smaller set of standing photographs. In this context it should be mentioned that a layer-line screen has not only the simple function of a selecting diaphragm, but the gap width determines the resolution volume within which diffuse intensity is collected (Welberry, 1983). For further discussion of questions of resolution see below. Single-crystal diffractometer measurements, either in the X-ray or in the neutron case, are frequently adopted for quantitative measurements of diffuse intensities. Microdensitometer recording of X-ray films is an equivalent method, incorporating corrections for background and other factors into this procedure. A comparison of Weissenberg and diffractometer methods for the measurement of diffuse scattering is given by Welberry & Glazer (1985).

In the case of powder-diffractometer experiments preferred orientations/textures could lead to a complete misidentification of the problem. Single-crystal experiments are preferable in some respect, because diffuse phenomena in a powder diagram may be analysed only after an idea about the disorder has been obtained and only in special cases. Nevertheless, high-resolution powder investigations give quick supporting information, *e.g.* about superlattice peaks, split reflections, lattice strains, domain size effects, lattice-constant change related to a disorder effect *etc.*

Before starting an experiment of any kind, one should specify the optimum wavelength. This is important with respect to the problem to be solved: *e.g.*, point defects cause diffuse scattering to fall off with increasing scattering vector; short-range ordering between clusters causes broad peaks corresponding to large d spacings; lattice-relaxation processes induce a broadening of the interferences (Huang scattering); or static modulation waves with long periods give rise to satellite scattering close to Bragg peaks. In all these cases a long wavelength is preferable. On the other hand, a shorter wavelength is needed if diffuse phenomena are structured in a sense that broad peaks are observable up to large reciprocal vectors, or diffuse streaks or planes have to be recorded up to high values of the scattering vector in order to decide between different models. The λ^3-dependence of the scattered intensity, in the framework of the kinematical theory, is a crucial point for exposure or data-acquisition times. Moreover, the accuracy with which an experiment can be carried out suffers from a short wavelength: generally, momentum as well as energy resolution are lower. For a quantitative estimate detailed considerations of resolution in reciprocal (and energy) space are needed. Special attention must be paid to absorption phenomena, in particular when (in the X-ray case) an absorption edge of an element of the sample is close to the wavelength used. $\lambda \sim 0.91$ Å must be avoided in combination with film methods owing to the K edge of Br. Strong fluorescence scattering may completely obscure weak diffuse-scattering phenomena. In comparison with X-rays, the generally lower absorption coefficients of neutrons of any wavelength makes absolute measurements easier. This also allows the use of larger sample volumes, which is not true in the X-ray case. An extinction problem does not exist in diffuse-scattering work. In particular, the use of a long wavelength is profitable when the main diffuse contributions can be recorded within an Ewald sphere as small as the Bragg cut-off of the sample: $\lambda = 2d_{\max}$; a contamination by Bragg scattering can then be avoided.

This is also advantageous from a different point of view: because the contribution of thermal diffuse scattering increases with increasing scattering vector $\mathbf{H}$, the relative amount of this component becomes negligibly small within the first reciprocal cell.

Highly monochromatic radiation should be used in order to eliminate broadening effects due to the wavelength distribution. Focusing monochromators help to overcome the lack of luminosity. A focusing technique, in particular a focusing camera geometry, is very helpful for deciding between geometrical broadening and 'true' diffuseness. With good success a method is used where in a monochromatic divergent beam the sample is placed with its selected axis lying in the scattering plane of the monochromator (Jagodzinski, 1968). The specimen is fully embedded in the incident beam which is focused onto the film. By this procedure the influence of the sample size is suppressed in one dimension. In an oscillation photograph a high resolution perpendicular to the diffuse layer lines may thus be achieved.

A serious problem is a careful suppression of background scattering. Incoherent X-ray scattering as an inherent property of a sample occurs as continuous blackening in the case of fluorescence, or as scattering at high 2θ angles owing to Compton scattering or 'incoherent' inelastic effects. Protecting the film by a thin Al or Ni foil is of some help against fluorescence, but also attenuates the diffuse intensity. Scratching the film emulsion after the exposure from the 'front' side of the film is another possibility for reducing the relative amount of the lower-energy fluorescence radiation. Obviously, energy-dispersive counter methods are highly efficient in this case (see below). Air scattering produces a background at low 2θ angles which may easily be avoided by special slit systems and evacuation of the camera.

In X-ray or neutron diffractometer measurements incoherent and multiple scattering contribute to a background which varies only slowly with 2θ and can be subtracted by linear interpolation or fitting a smooth curve, or can even be calculated quantitatively and then subtracted. In neutron diffraction there are rare cases when monoisotopic and 'zero-spin' samples are available and, consequently, the corresponding incoherent scattering part vanishes completely. In some cases a separation of coherent and incoherent neutron scattering is possible by polarization analysis (Gerlach *et al.*, 1982). An 'empty' scan can take care of instrumental background contributions. Evacuation or controlled-atmosphere studies need a chamber which may give rise to spurious scattering. This can be avoided if no part of the vacuum chamber is hit by the primary beam. The problem is less serious in neutron work. Mounting a specimen, *e.g.*, on a silica fibre with cement, poorly aligned collimators or beam catchers are further sources. Sometimes a specimen has to be enclosed in a capillary which will always be hit by the incident beam. Careful and tedious experimental work is necessary in the case of low- and high-temperature (or -pressure) investigations which have to be carried out in many disorder problems. Whereas the experimental situation is again less serious in neutron scattering, there are large problems with scattering from

walls and containers in X-ray work. Most of the X-ray investigations have therefore been made on quenched samples. Because TDS is dominating at high temperatures, also in the presence of a static disorder problem, the quantitative separation can hardly be carried out in the case of high experimental background. Calculation and subtraction of the TDS is possible in principle, but difficult in practice.

A quantitative analysis of diffuse-scattering data is essential for a definite decision about a disorder model. By comparison of calculated and corrected experimental data the magnitudes of the parameters of the structural disorder model may be derived. A careful analysis of the data requires, therefore, corrections for polarization (X-ray case), absorption and resolution. These may be performed in the usual way for polarization and absorption. Very detailed considerations, however, are necessary for the question of instrumental resolution which depends, in addition to other factors, on the scattering angle and implies intensity corrections analogous to the Lorentz factor used in structure analysis from sharp Bragg reflections.

Resolution is conveniently described by a function, $R(\mathbf{H}-\mathbf{H}_0)$, which is defined as the probability of detecting a photon or neutron with momentum transfer $h\mathbf{H} = h(\mathbf{k}-\mathbf{k}_0)$ when the instrument is set to measure $\mathbf{H}_0$. This function R depends on the instrumental parameters (collimations, mosaic spread of monochromator, scattering angle) and the spectral width of the source. Fig. 4.2.5.1 shows a schematic sketch of a diffractometer setting. Detailed considerations of resolution volume in X-ray diffractometry are given by Sparks & Borie (1966). If a triple-axis (neutron) instrument is used, for example in a purely elastic configuration, the set of instrumental parameters is extended by the mosaic of the analyser and the collimations between analyser and detector (see Chapter 4.1).

If photographic (X-ray) techniques are used, the detector aperture is controlled by the slit width of the microdensitometer. A general formulation of R in neutron diffractometry is given by Cooper & Nathans (1968):

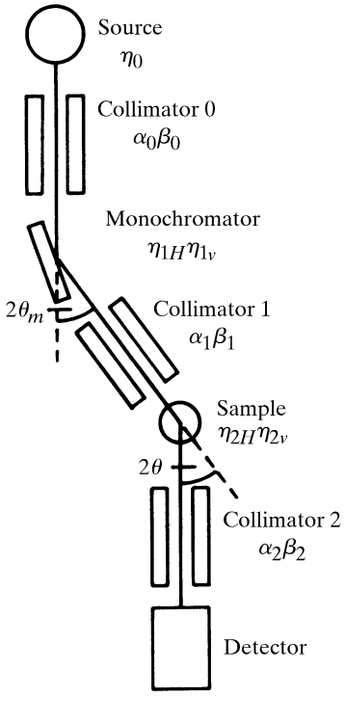

Fig. 4.2.5.1. Schematic sketch of a diffractometer setting.

$$R'(\mathbf{H}-\mathbf{H}_0) = R'_0 \exp\left\{-\tfrac{1}{2}\sum_k \sum_l M'_{kl}\Delta H_k \Delta H_l\right\}. \qquad (4.2.5.1)$$

Gaussians are assumed for the mosaic distributions and for the transmission functions the parameters are involved in the coefficients R'_0 and M'_{kl}.

The general assumption of Gaussians is not too serious in the X-ray case (Iizumi, 1973). Restrictions are due to absorption which makes the profiles asymmetric. Box-like functions are considered to be better for the spectral distribution or for large apertures (Boysen & Adlhart, 1987). These questions are treated in some detail by Klug & Alexander (1954). The main features, however, may also be derived by the Gaussian approximation. In practice the function R may be obtained either by calculation from the known instrumental parameters or by measuring Bragg peaks of a perfect unstrained crystal. In the latter case [*cf.* equation (4.2.5.2)] the intensity profile is given solely by the resolution function. A normalization with the Bragg intensities is also useful in order to place the diffuse-scattering intensity on an absolute scale.

In single-crystal diffractometry the measured intensity is given by the convolution product of $\mathrm{d}\sigma/\mathrm{d}\Omega$ with R,

$$I(\mathbf{H}_0) = \int \frac{\mathrm{d}\sigma}{\mathrm{d}\Omega}(\mathbf{H}) \cdot R(\mathbf{H}-\mathbf{H}_0)\,\mathrm{d}\mathbf{H}, \qquad (4.2.5.2)$$

where $\mathrm{d}\sigma/\mathrm{d}\Omega$ describes the scattering cross section for the disorder problem. In more accurate form the mosaic of the sample has to be included:

$$I(\mathbf{H}_0) = \int \frac{\mathrm{d}\sigma}{\mathrm{d}\Omega}(\mathbf{H}-\Delta\mathbf{k}) \cdot \eta(\Delta\mathbf{k}) R(\mathbf{H}-\mathbf{H}_0)\,\mathrm{d}\mathbf{H}\,\mathrm{d}(\Delta\mathbf{k})$$
$$= \int \frac{\mathrm{d}\sigma}{\mathrm{d}\Omega}(\mathbf{H}') \cdot R'(\mathbf{H}'-\mathbf{H}_0)\,\mathrm{d}\mathbf{H}'. \qquad (4.2.5.2a)$$

$R'(\mathbf{H}'-\mathbf{H}_0) = \int \eta(\Delta\mathbf{k}) R(\mathbf{H}'+\Delta\mathbf{k}-\mathbf{H}_0)\,\mathrm{d}(\Delta\mathbf{k})$. $\eta(\Delta\mathbf{k})$ describes the mosaic block distribution around a most probable vector $\mathbf{k}_0$: $\Delta\mathbf{k} = \mathbf{k}-\mathbf{k}_0$; $\mathbf{H}' = \mathbf{H}-\Delta\mathbf{k}$.

In formulae (4.2.5.1) and (4.2.5.2) all factors independent of 2θ are neglected. All intensity expressions have to be calculated from equations (4.2.5.2) or (4.2.5.2*a*). In the case of a dynamical disorder problem, *i.e.* when the differential cross section also depends on energy transfer $\hbar\omega$, the integration must be extended over energy.

The intensity variation of diffuse peaks with 2θ was studied in detail by Yessik *et al.* (1973). In principle all special cases are included there. In practice, however, some important simplifications can be made if $\mathrm{d}\sigma/\mathrm{d}\Omega$ is either very broad or very sharp compared with R, *i.e.* for Bragg peaks, sharp streaks, 'thin' diffuse layers or extended 3D diffuse peaks (Boysen & Adlhart, 1987).

In the latter case the cross section $\mathrm{d}\sigma/\mathrm{d}\Omega$ may be treated as nearly constant over the resolution volume so that the corresponding 'Lorentz' factor is independent of 2θ:

$$L_{3D} = 1. \qquad (4.2.5.3)$$

For a diffuse plane within the scattering plane with very small thickness and slowly varying cross section within the plane, one derives for a point measurement in the plane:

$$L_{2D,\parallel} = (\beta_1'^2 + \beta_2^2 + \eta_{2v}^2 - \sin^2\theta)^{-1/2}, \qquad (4.2.5.4)$$

exhibiting an explicit dependence on θ ($\beta'_1, \beta_2, \eta_{2v}$ determining an effective vertical divergence before the sample, the divergence before the detector and the vertical mosaic spread of the sample, respectively).

In the case of *relaxed* vertical collimations $\beta'_1, \beta_2 \gg \eta_{2v}$

$$L_{2D,\parallel} = (\beta_1'^2 + \beta_2^2)^{-1/2}, \qquad (4.2.5.4a)$$

i.e. again independent of θ.

Scanning across the diffuse layer in a direction perpendicular to it one obtains an integrated intensity which is also independent of 2θ. This is even true if approximations other than Gaussians are used.

If, on the other hand, an equivalent diffuse plane is positioned perpendicular to the scattering plane, the equivalent expression for $L_{2D,\perp}$ of a point measurement is given by

$$\begin{aligned} L_{2D,\perp} \simeq [&4\eta_{2H}^2 \sin^2\theta\cos^2\psi + \alpha_2^2\sin^2(\psi-\theta) \\ &+ \sin^2(\psi+\theta) + 4\eta_0'\sin^2\theta\sin^2\psi \\ &- 4\alpha_1''\sin\theta\sin\psi\sin(\theta+\psi)], \end{aligned} \tag{4.2.5.5}$$

where ψ gives the angle between the line of intersection between the diffuse and the scattering plane and the vector $\mathbf{H}_0$. The coefficients η_{2H}, α_2, α_1', α_1'', η are either instrumental parameters or functions of them, defining horizontal collimations and mosaic spreads. In the case of a (sharp) X-ray line (produced, for example, by filtering) the last two terms in equation (4.2.5.5) vanish.

The use of integrated intensities from individual scans perpendicular to the diffuse plane, now carried out within the scattering plane, again gives a Lorentz factor independent of 2θ.

In the third fundamental special case, diffuse streaking along one reciprocal direction within the scattering plane (narrow cross section, slowly varying intensity along the streak), the Lorentz factor for a point measurement may be expressed by the product

$$L_{1D,\parallel} \simeq L_{2D,\parallel} L_{2D,\perp}, \tag{4.2.5.6}$$

where ψ now defines the angle between the streak and $\mathbf{H}_0$. The integrated intensity taken from an H scan perpendicular to the streak has to be corrected by a Lorentz factor which is equal to $L_{2D,\parallel}$ [equation (4.2.5.4)]. In the case of a diffuse streak perpendicular to the scattering plane a relatively complicated equation holds for the corresponding Lorentz factor (Boysen & Adlhart, 1987). Again more simple expressions hold for integrated intensities from H scans perpendicular to the streaks. Such scans may be performed in the radial direction (corresponding to a θ–2θ scan):

$$L_{1D,\perp,\mathrm{rad}} = (4\eta_{2H}^2 + \alpha_2^2 + \alpha_1'^2)^{-1/2} \cdot 1/\sin\theta \tag{4.2.5.7}$$

or perpendicular to the radial direction (within the scattering plane) (corresponding to an ω scan):

$$L_{1D,\perp,\mathrm{per}} = (\alpha_2^2 + \alpha_1^2 + 4\eta_0'\tan^2\theta - 4\alpha_1''\tan\theta)^{-1/2} \cdot 1/\cos\theta \tag{4.2.5.8}$$

Note that only the radial scan yields a simple θ dependence ($\sim 1/\sin\theta$).

From these considerations it is recommended that integrated intensities from scans perpendicular to a diffuse plane or a diffuse streak should be used in order to extract the disorder cross sections. For other scan directions, which make an angle α with the intersection line (diffuse plane) or with a streak, the L factors are simply: $L_{2D,\perp}/\sin\alpha$ and $L_{1D,\perp}/\sin\alpha$, respectively.

One point should be emphasized: since in a usual experiment the integration is performed over an angle $\Delta\omega$ *via* a general $\delta\omega : (g\delta 2\theta)$ scan, an additional correction factor arises:

$$\Delta\omega/\Delta\mathbf{H}_\beta = \sin(\beta+\theta)/(\mathbf{k}_0\sin 2\theta). \tag{4.2.5.9}$$

β is the angle between $\mathbf{H}_0$ and the scan direction $\mathbf{H}_\beta$; $g = (\tan\beta + \tan\theta)/(2\tan\theta)$ defines the coupling ratio between the rotation of the crystal around a vertical axis and the rotation of the detector shaft. Most frequently used are the so-called 1:2 and ω-scan techniques where $\beta = 0$ and 90°, respectively.

It should be mentioned that the results in the neutron case are restricted to the elastic diffuse part, since in a diffractometer measurement the inelastic part deserves special attention concerning the integration over energy by the detector (Tucciarone *et al.*, 1971; Grabcev, 1974). If a triple-axis instrument is used, the collimations α_2 and β_2 have to be replaced by effective values after the sample owing to the analyser system.

In order to optimize a single-crystal experiment, the scan direction and also the instrumental collimations should be carefully chosen according to the anisotropy of the diffuse phenomenon. If the variation of $\mathrm{d}\sigma/\mathrm{d}\Omega$ is appreciable along a streak, the resolution should be held narrow in one direction and relaxed in the other to gain intensity and the scans should be performed perpendicular to that direction. If the variation is smooth the sharpest signal is measured by a scan perpendicular to the streak. In any case, a good knowledge of the resolution and its variation with 2θ is helpful.

Even the diffuse background in powder diagrams contains valuable information about disorder. Only in very simple cases can a model be deduced from a powder pattern alone; however, a refinement of a known disorder model can favourably be carried out, *e.g.* the temperature dependence may be studied. On account of the intensity integration the ratio of diffuse intensity to Bragg intensity is enhanced in a powder pattern. Moreover, a powder pattern contains, in principle, all the information about the sample and might thus reveal more than single-crystal work.

The quantitative calculation of a diffuse background is also helpful in combination with Rietveld's (1969) method for refining an averaged structure by fitting (powder) Bragg reflections. In particular, for highly anisotropic diffuse phenomena characteristic asymmetric line shapes occur.

The calculation of these line shapes is treated in the literature, mostly neglecting the instrumental resolution (see, *e.g.*, Warren, 1941; Wilson, 1949; Jones, 1949; and de Courville-Brenasin *et al.*, 1981). This is not justified if the variation of the diffuse intensity becomes comparable with that of the resolution function as is often the case in neutron diffraction. It may be incorporated by taking advantage of a resolution function of a powder instrument (Caglioti *et al.*, 1958). A detailed analysis of diffuse peaks is given by Yessik *et al.* (1973), the equivalent considerations for diffuse planes and streaks by Boysen (1985). The case of 3D random disorder (incoherent neutron scattering, monotonous Laue scattering, averaged TDS, multiple scattering or short-range-order modulations) is treated by Sabine & Clarke (1977).

In polycrystalline samples the cross section has to be averaged over all orientations (n_c = number of crystallites in the sample):

$$\frac{\mathrm{d}\sigma_p}{\mathrm{d}\Omega}(\mathbf{H}') = \frac{n_c}{H^2}\int \frac{\mathrm{d}\sigma}{\mathrm{d}\Omega}(\mathbf{H}')R'(|\mathbf{H}'| - |\mathbf{H}_0|)\,\mathrm{d}\mathbf{H}' \tag{4.2.5.10}$$

and this averaged cross section enters the relevant expressions for the convolution product with the resolution function.

A general intensity expression may be written as (Yessik *et al.*, 1973):

$$I_n(\mathbf{H}_0) = P\sum_\tau m(\tau)A_n\Phi_n(\mathbf{H}_0,\tau). \tag{4.2.5.11}$$

P denotes a scaling factor depending on the instrumental luminosity, τ the shortest distance to the origin of the reciprocal lattice, $m(\tau)$ the corresponding symmetry-induced multiplicity, A_n contains the structure factor of the structural units and the type of disorder, and Φ_n describes the characteristic modulation of the diffuse phenomenon of dimension n in the powder pattern. These expressions are given below with the assumption of Gaussian line shapes of width D for the narrow extension(s). The formulae depend on a factor $M = A_{1/2}(4k_1^2 - H_0^2)/(32\ln 2)$, where $A_{1/2}$ describes the dependence of the Bragg peaks on the instrumental parameters U, V, W (see Caglioti *et al.*, 1958),

$$A_{1/2}^2 = U\tan^2\theta + V\tan\theta + W. \tag{4.2.5.12}$$

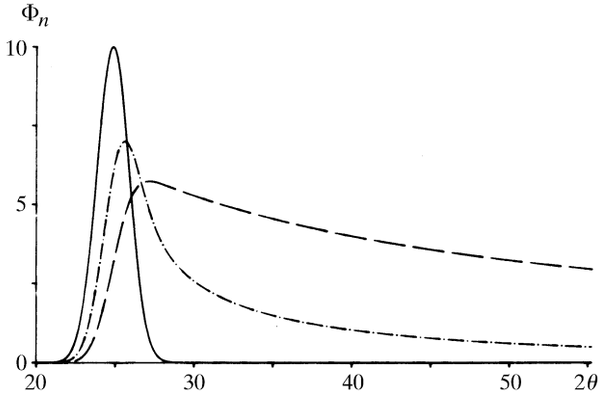

Fig. 4.2.5.2. Line profiles in powder diffraction for sharp and diffuse reflections; peaks (full line), continuous streaks (dot–dash lines) and continuous planes (broken lines). For explanation see text.

(*a*) *Isotropic diffuse peak around* τ

$$\Phi_0 = [2\pi(M^2 + D^2)]^{-1/2} \cdot 1/\tau^2 \times \exp\{-(\mathbf{H}_0 - \tau)^2/2(M^2 + D^2)\}. \quad (4.2.5.13)$$

The moduli $|\mathbf{H}_0|$ and $|\tau|$ enter the exponential, *i.e.* the variation of $d\sigma/d\Omega$ along $|\mathbf{H}_0|$ is essential. For broad diffuse peaks ($M \ll D$) the angular dependence is due to $1/\tau^2$, *i.e.* proportional to $1/\sin^2\theta$. This result is valid for diffuse peaks of any shape.

(*b*) *Diffuse streak*

$$\Phi_1 = 2\pi(M^2 + D^2)^{-1/2} \int (\tau^2 + q^2)^{-1/2} \times \exp\{-\mathbf{H}_0 - \sqrt{\tau^2 + q^2}/2(M^2 + D^2)\}\, dq. \quad (4.2.5.14)$$

The integral has to be evaluated numerically. If $(M^2 + D^2)$ is not too large, the term $1/k_0^2 = 1/(\tau^2 + q^2)$ varies only slowly compared to the exponential term and may be kept outside the integral, setting it approximately to $1/H_0^2$.

(*c*) *Diffuse plane (with* $r^2 = q_x^2 + q_y^2$*)*

$$\Phi_2 = (M^2 + D^2)^{-1/2} \int r^2/(\tau^2 + r^2) \times \exp\{-\mathbf{H}_0 - \sqrt{\tau^2 + r^2}/2(M^2 + D^2)\}\, dr. \quad (4.2.5.15)$$

With the same approximation as in (*b*) the expression may be simplified to

$$\Phi_2 = \pi/\mathbf{H}_0[1 - \mathrm{erf}\{(\tau - \mathbf{H}_0)/\sqrt{2(M^2 + D^2)}\} + 1/\mathbf{H}_0^2\sqrt{2\pi(M^2 + D^2)} \times \exp\{-(\mathbf{H}_0 - \tau)^2/2(M^2 + D^2)\}]. \quad (4.2.5.16)$$

(*d*) *Slowly varying diffuse scattering in three dimensions*

$\Phi_3 =$ constant.

Consequently, the intensity is directly proportional to the cross section. The characteristic functions Φ_0, Φ_1 and Φ_2 are shown in Fig. 4.2.5.2 for equal values of τ and D. Note the relative peak shifts and the high-angle tail.

Techniques for the measurement of diffuse scattering using a *white* spectrum are common in neutron diffraction. Owing to the relatively low velocity of thermal or cold neutrons, time-of-flight (TOF) methods in combination with time-resolving detector systems, placed at a fixed angle 2θ, allow for a simultaneous recording along a radial direction through the origin of reciprocal space (see, *e.g.*, Turberfield, 1970; Bauer *et al.*, 1975). The scan range is limited by the Ewald spheres corresponding to λ_{max} and λ_{min}, respectively. With several such detector systems placed at different angles, several scans may be carried out simultaneously during one neutron pulse. There is a renaissance of these methods in combination with high-flux pulsed neutron sources.

An analogue of neutron TOF diffractometry in the X-ray case is a combination of a white source of X-rays and an energy-dispersive detector. This technique, which has been known in principle for a long time, suffered from relatively weak white sources. With the development of high-power X-ray generators or the powerful synchrotron source this method has become highly interesting in recent times. Its use in diffuse-scattering work (in particular, resolution effects) is discussed by Harada *et al.* (1984).

Valuable developments with a view to diffuse-scattering work are multidetectors (see, *e.g.*, Haubold, 1975) and position-sensitive detectors for X-rays (Arndt, 1986*a*) and neutrons (Convert & Forsyth, 1983). A linear position-sensitive detector allows one to record a large amount of data at the same time, which is very favourable in powder work and also in diffuse scattering with single crystals. By combining a linear position-sensitive detector and the TOF method a whole area in reciprocal space is accessible simultaneously (Niimura *et al.*, 1982; Niimura, 1986). At present, area detectors are mainly used in combination with low-angle scattering techniques, but are also of growing interest for diffuse-scattering work (Arndt, 1986*b*).

references